Nano Energy 108 (2023) 108168

Contents lists available at ScienceDirect

Nano Energy

journal homepage: www.elsevier.com/locate/nanoen

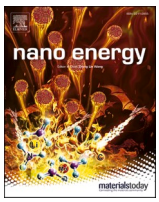

Edible cellulose-based conductive composites for triboelectric nanogenerators and supercapacitors

Leonardo Lamanna [a,b,*], Giuseppina Pace [b,c,**], Ivan K. Ilic [b], Pietro Cataldi [b,d], Fabrizio Viola [b], Marco Friuli [a], Valerio Galli [b,e], Christian Demitri [a], Mario Caironi [b,***]

[a] Department of Engineering for Innovation, Campus Ecotekne, University of Salento, Via per Monteroni, 73100 Lecce, Italy
[b] Center for Nano Science and Technology @PoliMi, Istituto Italiano di Tecnologia, Via G. Pascoli, 70/3, Milano 20133 Italy
[c] Institute for Microelectronics and Microsystems - National Research Council (IMM-CNR), Via C. Olivetti 2, 20864 Agrate, Milan, Italy
[d] Smart Materials Group, Istituto italiano di Tecnologia, via Morego 30, 16163 Genova, Italy
[e] Physics Department- Politecnico di Milano, piazza Leonardo da Vinci 32, 20133 Milan, Italy

ARTICLE INFO

Keywords:
Edible electronics
Green electronics
Triboelectric nanogenerators
Supercapacitors
Edible conductor
Ethyl cellulose

ABSTRACT

Edible electronics will enable systems that can be safely ingested and degraded in the human body after completing their function, such as sensing physiological parameters or biological markers in the gastrointestinal tract, without risk of retention or need of recollection. The same systems are potentially suitable for directly tagging food, monitoring its quality, and developing edible soft actuators control and sensing abilities. Designing appropriate edible power sources is critical to turn such a vision into real opportunities. We propose electrically conductive edible composites based on ethylcellulose and activated carbon as enabling materials for energy harvesting and storage. Free-standing, phase-separated bi-layered films, insulating at the top and with low electrical resistivity (~10 Ω cm) at the bottom, were produced with a scalable single-step process. Food additives can tune the mechanical and triboelectrical properties of the proposed edible films. We demonstrated their successful operation as electropositive elements in organic triboelectric nanogenerators (TENGs) and as electrodes in fully edible supercapacitors (SC). The TENGs showed ~60 V peak voltage (root mean square power density ~2.5 μW cm^{-2} at 5 Hz), while the SC achieved an energy density of 3.36 mW h g^{-1}, capacity of ~ 9 mAh $g^{-1,}$ and stability for more than 1000 charge-discharge cycles. These results show that the combination of ethyl cellulose and activated carbon, and the control over their mixture, allow on-demand edible devices for energy generation and storage, serving future edible and green electronics scenarios.

1. Introduction

The advancement in electronics is generating a variety of miniaturized and integrated circuits that are changing our lives in the form of robots and smart devices, with notable examples in medical diagnostics and treatments. Novel sensors and actuators, cardiac and gastric pacemakers, ingestible and edible pills are advancing medicine. [1–6] Such progress results in a continued need for high-performing, biocompatible and environmental friendly power supplies. However, efficient energy generation and storage still remain challenging for the sustainable operation of portable and implantable electronics. [7].

The power source of most of these devices relies on currently available batteries. This causes inconvenience both for patients, who may need a second operation to remove them, and for the environment, which is burdened with non-recyclable waste. [8] Often, such electronic waste comprises toxic and dangerous metals such as Li, Hg, Pb, Ni, and Cd and can lead to serious environmental issues when not properly disposed of. [9].

Therefore, there is an urgent need to develop environmentally-friendly, low-cost, lightweight, biocompatible, and efficient energy generation and storage solutions. Recently, nanogenerators, new-generation batteries, capacitors, and fuel cells were proposed as effective solutions to the above-described problems. However, most of these devices are fabricated using fossil-derived long-lasting polymers, thus

* Corresponding author at: Department of Engineering for Innovation, Campus Ecotekne, University of Salento, Via per Monteroni, 73100 Lecce, Italy.
** Corresponding author at: Center for Nano Science and Technology @PoliMi, Istituto Italiano di Tecnologia, Via G. Pascoli, 70/3, Milano 20133 Italy.
*** Corresponding author.
E-mail addresses: leonardo.lamanna@unisalento.it (L. Lamanna), giuseppina.pace@mdm.imm.cnr.it (G. Pace), mario.caironi@iit.it (M. Caironi).

https://doi.org/10.1016/j.nanoen.2023.108168
Received 18 November 2022; Received in revised form 23 December 2022; Accepted 2 January 2023
Available online 4 January 2023

contributing to micro-nano plastic pollution lethal to aquatic life. [10] Biobased and biodegradable materials are alternatives to oil-derived synthetic polymers, as they are sourced from living organisms and/or decomposed at the end of their lives by the action of living bacteria and fungi into eco-friendly residuals (water, carbon dioxide, and biomass). [11,12] In addition to this, edible functional materials are rising interest for future edible electronics, an emerging field that aims to develop devices safe for ingestion, which can be degraded within the body. [13–16] Edible devices could find applications in healthcare in humans and animals, and smart labels for food monitoring. [1,13,17] Once completed their function edible devices could act as nourishment for humans in emergencies while reducing the ecological footprint [18,19]. Such advances can at the same time spark the development of edible soft actuators, i.e. edible robots. [18,20].

Alongside energy generation from large-scale green sources (e.g. sun, wind), [21,22] energy-harvesting devices, such as piezoelectric nanogenerators (PENGs) and triboelectric nanogenerators (TENGs) are becoming crucial for powering miniaturized robots and medical devices. In particular, TENGs can provide a sustainable solution for harvesting the almost ubiquitous mechanical energy. [23,24] TENGs exploit the charge transfer, taking place upon friction, between an electropositive and an electronegative triboelectric material. TENGs have already demonstrated their capability in converting biomechanical energy such as heartbeat and respiratory motion. [25,26] On the other side, supercapacitors (SCs) are widely exploited energy storage components in medical devices [27–29] thanks to their low-cost, adjustable small size, and flexibility. [30].

In the last few years, the increased interest in TENGs and edible devices has led to exploring the triboelectric property of edible materials. [31–33] Food additives have been used to improve the triboelectric properties [34] of materials or in some cases, food (e.g., sandwich bread) has been used as a device component in TENGs [7]. Nevertheless, there are only a few examples of edible TENGs. [32,35,36] These generators commonly employ edible metals that are safely ingestible only in small amounts, require multiple production steps, and are not stable in a water-based environment. On the other side, just two edible SCs were previously reported. [29,37] Both works report activated carbon as the active material and gold as the current collector. Regarding the binder needed for the activated carbon electrodes, while Wang et al. used egg whites, Gao et al. used a mix of gelatin and sugar. Nevertheless, both binders are suboptimal, as 2/3 of the electrode mass were egg whites, and around 40% was the gelatin-sugar mixture. This amount is significantly larger than the binder content in state-of-the-art SCs (< 10%), reducing the electrodes conductivity and limiting the performance of the device. [38].

In this study, we propose electrically conductive edible composites of ethyl cellulose (EC) and activated carbon (AC) and we demonstrate their use in energy harvesting and storage devices, such as TENGs and SCs. EC is a biobased and biodegradable polysaccharide, derivative of cellulose, with ethylated repeating glucose units. It can be used as adhesive, filler, or binder and it easily forms films. [39,40] It is one of the few edible non-water-soluble polymers, classified as food additive E462 by the European Food Safety Authority (EFSA), with an acceptable daily intake of 660–900 mg/kg body weight per day. [41] Cellulose and its derivatives are commonly used in pharmaceutics and the food industry. [42–45] AC is an edible electronic conductor, classified as E153 by EFSA with an acceptable daily intake of 67–800 mg/ kg body weight per day. [13,46] AC is stable in the gastrointestinal tract and is neither absorbed nor metabolized but it is just excreted in the feces [47], its microporous structure is widely exploited as an adsorbent for environmental pollutants or chemicals in poisoning and overdoses. [46] Moreover, thanks to its slightly smoky taste and dark coloring it is used as additive in food (e.g. bread, pizza, pasta, and ice cream).

Compared with the state-of-the-art, here simple one-pot synthesis processes are proposed for the manufacturing of edible TENGs and SCs. Indeed, the fabrication of most of the TENGs and SCs require long multistep processes, often involving the use of toxic solvents and vacuum tools (e.g. metal evaporator). Here we present an organic edible TENG integrating an AC/EC bi-layered film obtained from a single-step solution casting. The bottom layer is rich of AC and is electrically conductive (resistivity, $\rho \sim 10$ Ω•cm), while the top layer is made of pure EC and has an insulating character. Moreover, different food additives have been added to modulate the mechanical and triboelectric properties of the device. TENGs showed a peak voltage, short circuit current, and instant peak power of 60 V, ~2 μA, and ~ 7 μWcm^{-2} (RMS power 2.5 μW cm^{-2} at 5 Hz), respectively. The same AC and EC were exploited, by means of a slightly modified fabrication process, to formulate an electrode allowing to realize fully edible SCs, achieving an energy density of 3.36 mW h g^{-1}, a capacity of ~9 mAh g^{-1} with a charging-discharging rate of 0.1 A g^{-1}. No significant loss in performance was observed upon 1000 cycles.

Overall, the proposed edible composites show low electrical resistivity, and mechanical flexibility. They enabled the development of energy harvesters and storage devices with appreciable figures of merits, thus showing concrete progress for future edible electronic systems, and sustainable technologies.

2. Results and discussion

Starting from edible materials, we targeted the realization of novel TENGs and SCs offering strategies for the development of fully edible energy harvesting and storage devices. In particular, we paid attention to the sustainability and non-toxicity of the preparation process, aiming at a scalable solution-based approach adopting only water and ethanol. The AC/EC composite films were fabricated by dispersing the AC in a solution of EC in ethanol. The AC/EC dispersion was then cast in a petri dish and the ethanol solvent was let dry, as described in Fig. 1a (see materials and methods for details). To improve the film flexibility, and reduce the film brittleness, we tested different edible additives, including food additives (citric acid - E330, and myristic acid – E570), and sunflower oil.

The casting process is accompanied by phase segregation of components, generating films with opposite faces showing completely different electrical properties: a conductive bottom layer rich in AC, where EC acts as a binder, [48] and a top layer consisting of pure EC (inset Fig. 1a).

The cross-section micromorphology of the films highlights the phase separation, which becomes more evident in samples with an AC content higher than 10% (fig. S1 in the Supporting Information, SI). With the addition of more AC filler, the thickness of the bottom conductive layer increases (fig. S1). SEM images of the bottom and top layer (Fig. 1b-c), show that even the bottom, AC rich layer is partially coated by a thin layer of EC. The top EC layer is instead uniform over its entire thickness as demonstrated by the SEM cross-section. This generates a slight difference in the wettability between bottom and top layers (contact angle reported in fig. S2) as the hydrophobicity of the AC layer increases the contact angle (from 63 ± 11° to 80 ± 12°).

In the absence of AC and at 5% of AC, the film resistance is above the instrument resolution limit (fig.S3). The percolation threshold, which can be defined as the minimum filler concentration required to effectively transport electronic charges among the conductive particles, [49,50] has been extracted from the current-voltage curves. Ohmic behavior, which demonstrates the filler interconnection, is almost reached with 10% AC filler content, as shown in fig.S3 (resistance variation is within 14% in the explored voltage range). The electrical sheet resistance was calculated and has been reported against the AC filler content in Fig. 1d. When the percolation threshold (10% AC) is reached, the sheet resistance is ~ 250 kΩ/sq. Upon increasing the filler content to 60%, the resistance drops to ~1 kΩ/sq. All the films with a concentration of AC filler above 10% have a similar resistivity of ~10 Ω cm (fig. S4). At 20% and above of AC filler, the percolation network is saturated, and the further addition of the conductive filler

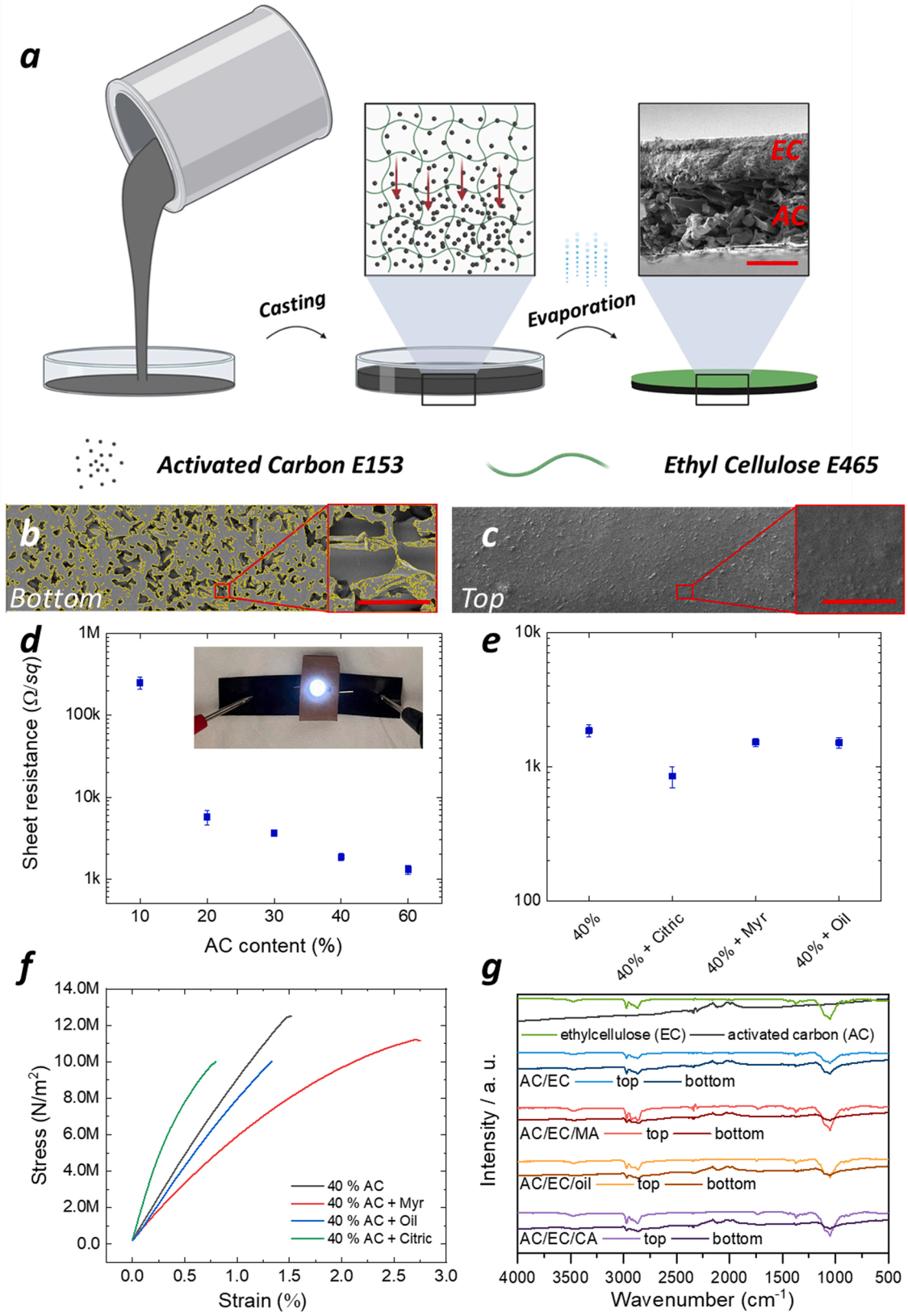

Fig. 1. a) Edible positive triboelectric film manufacturing. Ethanol-AC-EC slurry is drop cast in a petri dish and left to evaporate, AC precipitates, and a layered biphasic film is obtained, SEM cross-section image of 40% AC sample is reported in the inset (scale bar 35 μm); b,c) SEM images of bottom and top layer, respectively (scale bar 50 μm). EC edges on the bottom layer are highlighted; d) electrical resistance of the film as a function of the AC content. In the inset, the powering of a white LED through the conductive film, with 3 V applied; e) electrical resistance of the film with 40% of AC with different food additives; f) tensile stress-strain measurement of films with different additives; g) FTIR fingerprints of both layers of the films.

only increases the thickness of the conductive layer (fig. S1, S4). The obtained resistivity values are consistent with other reports that employ AC (range of resistivity 0.5–1000 Ω cm) [13,14]. The low resistance of the films enables to power up a light-emitting diode (LED) connected through the bottom layer of the film, as shown in the inset of Fig. 1d.

The addition of AC filler in the EC films not only provides electrical conductivity to the bottom layer of the samples but also modifies the film mechanical properties. Tensile strain properties are reported in fig. S5. A decrease in the Young modulus and maximum strain with the increase of the AC content is observed. Such behavior is due to a greater concentration of micro defects in the EC film as the AC content increases, promoting the breakup of the film under tension stress. [51,52].

Considering the data of sheet resistance, thickness, and mechanical properties obtained with the different amounts of AC, the 40% formulation has been chosen to further modulate the mechanical property by adding different food or food additives (Fig. 1e, fig S5, Fig. 1 f, and fig. S7). In particular, vegetable oil (sunflower oil), fatty acid (myristic acid) and flavoring/ preservative food (citric acid) were added (SEM cross-section image reported in fig. S6). The first two are EC plasticizers, [53–55] while citric acid is a cellulose cross linker [56,57] and AC modifier. [58,59] The ability to modify and tune the mechanical properties of the films by simply incorporating edible additives is interesting for the production of materials with multiple functionalities and easily adaptable to a specific application and surface [60,61].

As shown in Fig. 1e, the presence of additives does not affect the sheet resistance of the films. In contrast, the stress-strain curves are modified depending on the additive used (Fig. 1 f). In particular, the addition of oil and myristic acid improves the plasticity of the films, confirming the plasticizer effect of these materials. Myristic acid exhibited the strongest plasticizing effect, with an increase of the maximum sustained strain of ~105% and a reduction of the Young modulus by ~29% (fig. S7). Citric acid instead, has enhanced the stiffness of the films, increasing the Young modulus by ~101%, but reducing the maximum sustained stress and strain by ~10% and ~33%, respectively (fig. S7). Fourier transform infrared spectroscopy (FTIR) spectra were employed to obtain the chemical fingerprint of both layers of the films (Fig. 1 g; fig.S8 reports the FTIR spectra of all the pristine chemicals). The AC fingerprint peaks are not present on the top layer of the film, in agreement with the phase separation described above. Noteworthy, by analyzing the correlation between the AC spectrum and the bottom layer of the films, it was noticed that the addition of food additives improves the AC phase segregation at the bottom layer (fig. S9). Practical demonstrations of the different electrical properties of the films opposite layers (insulating vs conducting) and of the ability of the films to withstand bending and wrinkle stress were recorded on camera (Videos 1–3 in the Supporting Information).

For applications in the gastrointestinal (GI) tract, stability in GI fluids is the desired property. Thus, the edible films were immersed in simulated gastric fluid (SGF), and simulated intestinal fluid (SIF), and their weight was monitored for 72 h. Over such observation period, the films substantially maintained their original weight (fig. S10) and their asymmetry in the electrical properties of top and bottom layers, with a negligible variation of sheet resistance of the bottom layer. Such stability in SGF and SIF is promising for applications in ingestible and edible electronics. Indeed, cellulose is stable in the gastrointestinal tract and digested only in the large intestine by the bacterial flora. [62,63].

The above presented organic edible films were integrated into a demonstrative TENG to assess their suitability to work as the electropositive side of the harvesting device. In particular, the EC layer of the film acts as the electropositive triboelectric material and the AC layer as a carbon-based electrode. To realize the TENG, a reference negative triboelectric layer was used (Teflon), interfaced with an aluminum

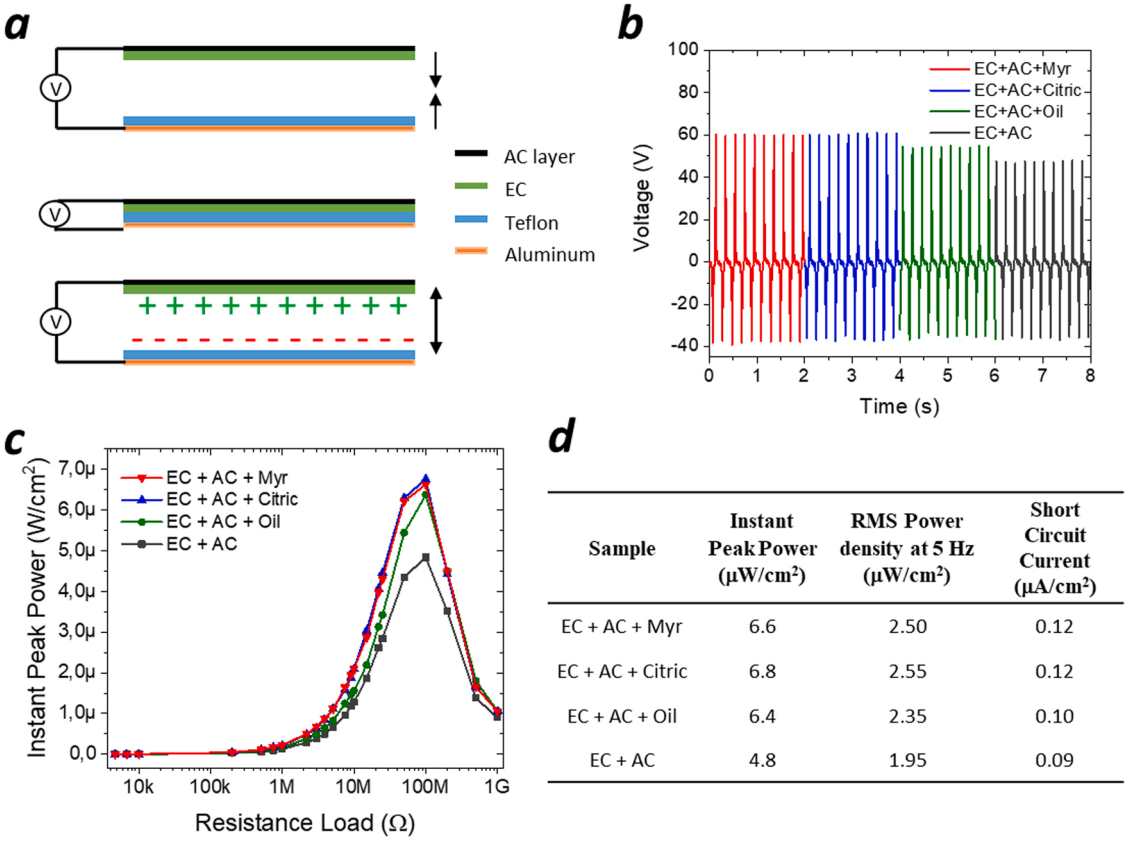

Sample	Instant Peak Power (μW/cm²)	RMS Power density at 5 Hz (μW/cm²)	Short Circuit Current (μA/cm²)
EC + AC + Myr	6.6	2.50	0.12
EC + AC + Citric	6.8	2.55	0.12
EC + AC + Oil	6.4	2.35	0.10
EC + AC	4.8	1.95	0.09

Fig. 2. a) Schematic of the TENGs structure operated in the contact-separation operation mode; b) Peak voltage measured with a 40 MΩ probe (force 10 N, 5 Hz, 5 mm air gap, area (4 ×4) cm^2); c) TENGs instant power output measured for the different films; d) table reporting the instant peak power maximum and the root mean square (RMS) power calculated for the different films.

electrode (Fig. 2a). TENGs with and active area of a 4 × 4 cm^2 were operated in contact-separation mode under an applied force of 10 N, motion frequency of 5 Hz and air gap of 5 mm. The stability of the TENGs was verified for 1000 cycles (fig. S11), moreover, the devices were tested at different distances, forces, and frequencies to evaluate the dependence from these parameters (fig. S12). The applied cycling mechanical input led to the generation of an AC voltage (probed with a 40 MΩ resistance load) followed by an AC current flowing through the external circuit. The comparison of the time dependent voltage, measured for TENGs fabricated with the different additives, is reported in Fig. 2b. Higher instant peak power output (Fig. 2c and Table 1) was found for TENGs in which the edible film contains additives (citric acid, myristic acid and oil, with 6.8, 6.6 μW/cm^2 and 6.4 μW/cm^2, respectively) with respect to the one without additives (4.8 μW/cm^2). This evidence shows that the additives not only impact the mechanical properties of the films reducing their brittleness, but they also affect the TENGs electrical performance. Such tuning of the performance is likely related to the fine phase segregation between the AC and EC components upon inclusion of an additive, as evidenced by FTIR data and relative spectra correlation (fig. S9). Table 1 reports a comparison of our TENG with other edible devices reported in the literature to date.

After demonstrating the possibility to adapt our edible composite films in an energy harvesting device, we turned to assess their properties in a relevant energy storage device, the supercapacitor. In particular, by exploiting the AC/EC composite (90:10 wt ratio) for the electrodes, we fabricated a fully edible SC (Fig. 3a). The AC, which is exploited for its high surface area allowing an increase of capacitance, does not have sufficient conductivity to support the transport of electrons. To overcome this limitation we used as current collector edible gold leafs [65]. Edible gold leaf was transferred onto ~50 μm thick pure EC film. Then, the gold layer was coated with the AC/EC composite (fig. S13). The use of food additives was not considered in this study, since it was verified that no change in the electrical conductivity is obtained with their addition (Fig. 1e). A nori algae separator was soaked in an aqueous electrolyte solution (Na_2SO_4 in water, 1 M) and was then sandwiched between the two electrodes. The full structure was encapsulated in beeswax to avoid solvent evaporation and to improve the SC stability over time (detail on SC fabrication in materials and methods). The developed SC cell showed close-to-ideal behavior in cyclic voltammetry tests (Fig. 3b). Different scan rates have been explored ranging from 5 mVs^{-1} to 100 mV s^{-1} showing excellent rate capability and stability of the fully edible SC. Furthermore, the electrochemical performance was studied via galvanostatic current charge and discharge tests. Linear voltage vs. time curves, showing almost perfect triangles, can be observed in Fig. 3c, indicating the formation of an electric double layer. The capacity retention has been calculated for different current densities: 0.1, 0.5, 2, and 10 A g^{-1} for 5 cycles each (Fig. 3d). A complete charge and discharge cycle could occur in less than 2 s at 10 A g^{-1}. A capacitance of 40, 34.4, 27.1, and 10.1 F g^{-1} has been calculated for a current density of 0.1, 0.5, 2, and 10 A g^{-1}, respectively. The maximum capacity of ~9 mAh g^{-1} has been observed with a current density of 0.1 A g^{-1}, which reduces with the increase in current densities. The calculated energy density is 3.36 mW h g^{-1} which is approximately one third of a commercial supercapacitor [66]. Switching back to the initial current density value of 0.1 A g^{-1}, the capacities reached the same values obtained in the first 5 cycles (Fig. 3d), indicating that no damage occurred at higher current densities [67]. The cyclic stability of the edible SC was assessed via a repeated charging-discharging test for 1000 cycles at a constant current density of 0.5 A g^{-1} (Fig. 3e). The device showed excellent stability for all the cycles with preservation of the original capacity. To further verify the stability of the edible SC, micromorphology SEM images of the composite electrode were taken before and after 1000 cycles (fig. S14), which demonstrated no apparent change in the microstructure. Table 2 reports a comparison of our SC with other edible devices reported in the literature to date.

The direct charging of the edible SC with an edible TENG cannot be achieved straightforwardly due to the high current necessary to charge the SC (up to 100 μA in DC), which would than require the development of a dedicated power management circuit. However, we show in fig. S15 that it is possible to charge a capacitor with our edible TENG.

3. Conclusion

In this work we proposed electrically conductive edible composites based on ethylcellulose, activated carbon and food additives. A simple and scalable single-step process was adopted to prepare free-standing bi-layered films that present an insulating top layer and a conductive bottom layer with an electrical resistivity as low as ~10 Ω cm. We showed the possibility to tune their mechanical and electrical properties by adding different amounts of food additives, including citric acid (E330), myristic acid (E570), and sunflower oil.

We successfully demonstrated the use of these edible conductors as electrodes in energy harvesting and storage devices, aiming at fulfilling the need of power sources in future edible and sustainable electronic systems. In particular, we adopted them to realize edible positive electrodes in triboelectric nanogenerators, achieving a maximum power output of ~2.5 μW/cm^2 at 5 Hz. With a simple modification of the formulation, we used the same composites as electrodes in a completely edible supercapacitor, stable for more than 1000 charge/discharge cycles, providing an energy density of 3.36 mW h g^{-1} and a maximum capacity of ~9 mAh g^{-1}.

The presented results offer new opportunities in edible electronics, expanding the library of edible conductors with composites that can be modulated in their composition to serve specific needs. Their use as electrodes in edible energy harvesting and storage devices with promising figures of merits, combined with simple and scalable fabrication schemes, shows a concrete path to fulfill the energetic requirements of envisioned edible systems, from edible smart pills, to food tags and control units in edible actuators (e.g. TENGs and SC could work as a signal generator or power supply for an oscillator to be applied for the drug release monitoring via intrabody communication [1]).

4. Materials and methods

Materials: Ethyl cellulose – E 465 (48–49.5 w/w ethoxyl basis), citric acid - E330, myristic acid – E570, and beeswax E901 were bought from

Table 1
Comparison of edible TENGs present in the literature. Where available, operational condition of the TENGs has been reported (frequency, force, resistance load).

Metric	[32]	[35]	[36]	[64]	Our work
Reference	ICP-Sputtering – Lithography	Mixing and drop casting on gold leaf	Silver leaf-coated laver	Elettrospinning- silver leaf	Mixing and drop casting
Material	Organic and metal	Organic and metal	Organic and metal	Organic and metal	All organic
Area	2 cm^2	6.25 cm^2	4 cm^2	9 cm^2	16 cm^2
Open circuit	55 V (1 GΩ)	50 V (5 GΩ)	23 V(-)	3 V(-)	60 V (40 MΩ)
Short Circuit Current	0.6 μA	1 μA	315 nA	40 nA	1.9 μA
Instant Power	2.16 μW/cm^2 (1 Hz,-,-)	0.648 μW/cm^2 (-,8 N,-)	0.002 μW/cm^2 (-,-,-)	12 μW/cm^2 (2 Hz,-,-)	6.8 μW/cm^2 (5 Hz, 10 N, 5 mm)
RMS Power	-	-	-	-	2.5 μW/cm^2 (5 Hz, 10 N, 5 mm)

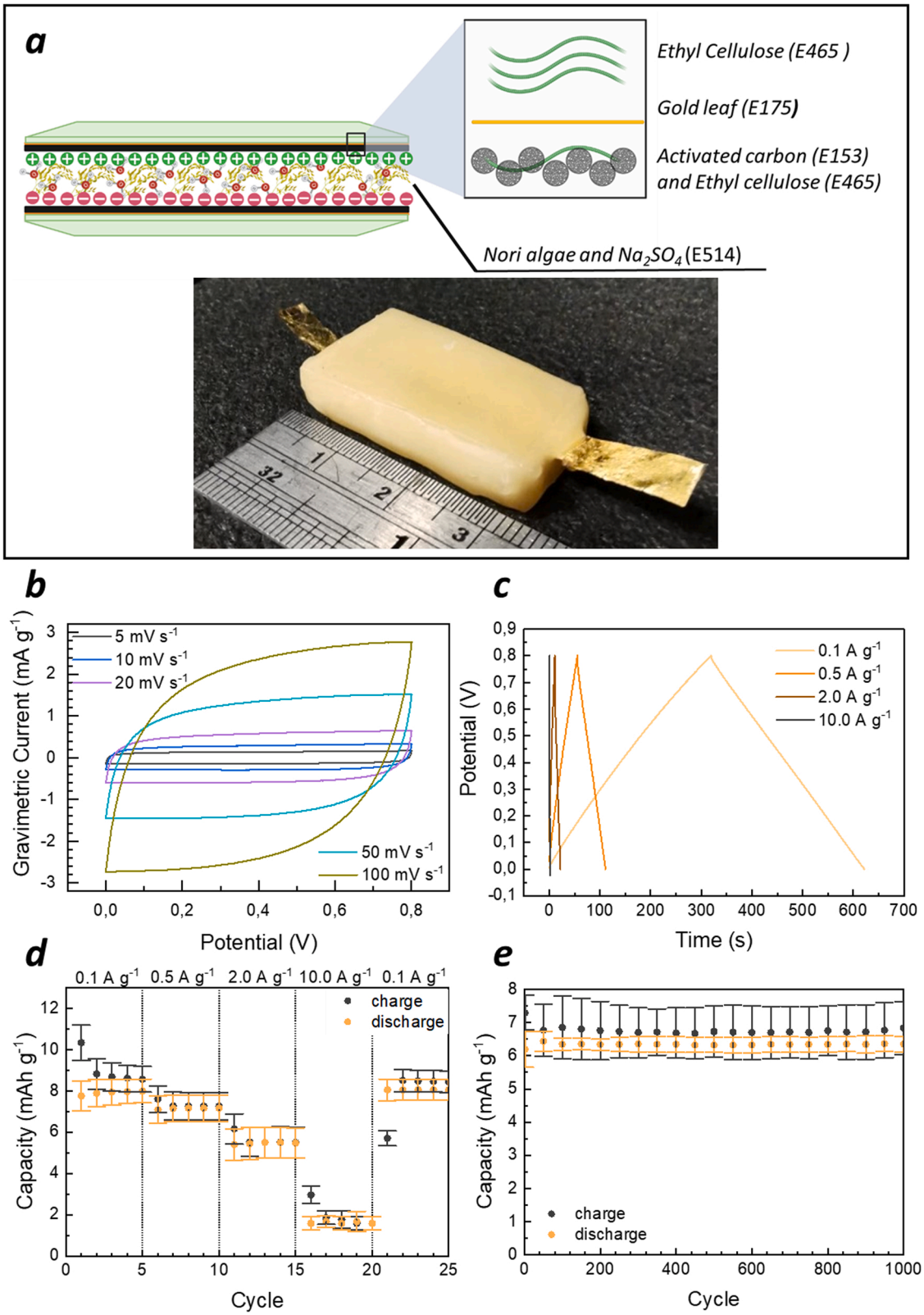

Fig. 3. (a) Scheme and a picture of the supercapacitor. (b) Cyclic voltammograms at different scan rates. (c) Galvanostatic charging-discharging curves at different current densities. (d) Capacities as calculated from galvanostatic charging-discharging tests at different current densities. (e) Capacities over 1000 cycles as calculated from galvanostatic charging-discharging tests at 0.5 A g^{-1}.

Table 2
Comparison of edible SCs present in the literature.

Metric	[37]	[29]	Our work
Mass (1 electrode)	80 mg	N/A	1.5 mg
Size (1 electrode)	16 cm^2	0.3 cm^2	1 cm^2
Binder	Egg white	Gelatin and sugar	Ethyl cellulose
Binder (%)	66.7	41.9	10
Electrolyte	Gatorade	Agar and monodosium glutamate	1 M Na_2SO_4
Shape of galvanostatic charging/ discharging	Almost triangular	Not triangular	Triangular
Capacitance	3.15 F @ 0.1 A g^{-1} (divided by 2 as the authors test it from −0.8 to 0.8 V)	23.6 mF @ 20 mV s^{-1}	40 F @ 0.1 A g^{-1}
Energy density	-	10.86 μW h cm^{-2}	3.36 mW h g^{-1}

Sigma Aldrich. Activated carbon for the bilayer conductive films used for the TENGs was purchased by the same supplier (Supelco, puriss. P.a., powder, E 153). Activated carbon for the SCs ink was purchased from Nature's Way under the name Charcoal, Activated (LOT: 21043 A). Sunflower Oil was bought in a supermarket. Edible gold leaf was bought from Kinno (thickness <500 nm). These materials were used as received without any further process needed.

TENGs films fabrication: EC was solubilized in ethanol (2% w/v) together with AC particle (from 0 to 60 wt% with respect to EC) and mixed overnight. 20 ml of solution was drop cast in 100 mm diameter glass Petri dishes, and the ethanol was allowed to evaporate at 50 °C. Such temperature has been chosen to avoid the coffee ring effect otherwise present. Different edible additives have been added at a concentration of 25% with respect to the EC (citric acid - E330, myristic acid – E570, and sunflower oil) to the solution to evaluate their influence on the mechanical and triboelectric properties. The dried films were cut in squares of 4 × 4 cm^2 and integrated in the TENGs. The data acquired on TENGs refer to films containing 40% AC, without any further processing.

Supercapacitor film manufacture process: EC films were prepared by solubilization in ethanol (2% w/v). One layer of the film was lightly wetted with ethanol, and a gold leaf was transferred to it. After a few hours of drying in air, the film was transferred in a vacuum chamber, where it was kept overnight. The current collectors were cut into stripes (0.5 mm wide) after drying. The stripes were coated with ethanol-based ink containing ethyl EC (2% w/v) and AC (18% w/v) so that 10 μL of the ink was deposited on 1 cm^2 of the stripe (2 cm from the edge). After drying the ink for 1 h in air at room temperatures, a 1 M Na_2SO_4 aqueous solution was added on top of the electrodes (20 μL each). The SC was assembled by adding the nori seaweed as a separator (previously immersed in the electrolyte) between the electrodes and sandwitched between two blocks of beeswax. Melted beeswax was poured on the edges of blocks to seal the device.

SGF was prepared as described in the United States Pharmacopoeia and consisted of a solution of 0.03 M NaCl adjusted at pH 1.2 with 1 M solution of HCl.

SIF was prepared as described in the United States Pharmacopoeia [68] and consisted of a solution of 0.05 M KH_2PO_4 adjusted at pH 6.8 with 0.2 molar solution of NaOH.

Degradation tests: Three different samples were immersed in the simulated gastrointestinal fluids at 37 °C, and their weight change monitored for 72 h.

FTIR: Infrared spectra of the films were collected through an attenuated total reflectance (ATR) accessory (Bruker-VERTEX 70 v FT-IR Spectrometer).

SEM analysis: SEM measurements were performed using a Tescan MIRA3 operating at an acceleration voltage of 2 kV and recording the secondary electron emission. The samples were prepared as here described. After immersion at − 195.79 °C in liquid nitrogen, the samples were cut by tearing them with two tweezers to preserve the original cross-section morphology and then pretreated by an ultra-thin (~10 nm) gold sputtering deposition.

The electrical resistance of the edible conductive films was measured by means of Semiconductor Parameter Analyzer Agilent B1500A. Silver paste (RS pro) was painted, forming 5 mm wide contacts spaced by 5 mm. Sheet resistance was acquired with a four-point-probes configuration. Resistivity was then calculated considering the described geometry and thickness of the samples.

Contact angle: Static water contact angles were measured on both layers of the film by an optical contact angle device (DataPhysics). 10 microliters of deionized water were deposited on the samples.

Mechanical tests: To determine the mechanical feature of the films a Zwick Roell was used, following the regulation ASTM D882. Samples were stretched by applying a strain rate of 20 mm min^{-1}.

TENG characterization: The TENG electrical characterization was performed with a home-built setup. The setup includes a linear motor and load cell, an oscilloscope (Tektronix MSO5000), a voltage probe 40 MΩ (Tektronix) for voltage measurements, a current amplifier (1211 DL Instruments) and a home-built resistance commutator for current measurements. The device's active area was 4 × 4 cm^2. The TENGs were operated in contact-release mode with an applied force of 10 N, operational frequency of 5 Hz and an airgap of 5 mm.

The instant peak power was extracted from the current peak maximum measured at varying the resistance loads ($P = R_{Load}\ I^2_{Peak}$). The RMS power was calculated according to the formula$P_{RMS} = \frac{1}{T}\int_0^T i^2 R_{Load} dt$, with T being the time interval of a full cycle at 5 Hz.

All data reported in the manuscript have been acquired after cycling each device at least 1000 time, ensuring long time stability under continuous mechanical stimuli. Output current measurement at varying resistance loads has been acquired right after the 1000 initial conditioning cycles and run for another 1000 cycles (i.e. the stability of the devices is guaranteed at least for 2000 cycles).

Supercapacitor characterization: SCs were tested on MultiPalmSens4 potentiostat and galvanostat in 2-electrode setup. The measurements were performed in triplicate and average with the standard error is shown. Cyclic voltammetry was performed firstly by at 5 mV s^{-1} for 10 cycles and then at 10, 20, 50, and 100 mV s^{-1} for 3 cycles each. The cyclic voltammogram of the last cycle is shown. 5 cycles of galvanostatic charging-discharging was performed at 0.1, 0.5, 5.0, and 10 A g^{-1} each and then again at 0.1 A g^{-1}. Charging-discharging curves of the last cycle at each current density are shown. Long term cycling was performed at 0.5 A g^{-1} for 1000 cycles.

Capacitances were calculated as:

$$C = \frac{q}{V}$$

Where q the charge held, and V is the electric potential.

Energy density was calculated as:

$$E_d = \frac{I_d}{7.2} Vt$$

where I_d is current density, V is the voltage window, and t is discharging time.

E_d of 3.36 Wh kg^{-1} has been calculated for discharging 0.1 A g^{-1}.

Statistical Analysis: The error bar are presented as mean ± standard deviation calculated on a minimum of three independent samples using the Excel or Origin software.

CRediT authorship contribution statement

Leonardo Lamanna: Conceptualization, Methodology, Formal

analysis, Visualization, Investigation, Data curation, Validation, Writing – original draft, **Giuseppina Pace**: Investigation, Methodology, Formal analysis, Validation, Draft review, **Ivan K Ilic:** Investigation, Methodology, Formal analysis, Validation, Draft review, **Pietro Cataldi:** Investigation, Methodology, Validation, Draft review, **Fabrizio Viola:** Investigation, **Marco Friuli:** Investigation, **Valerio Galli**: Investigation, **Christian Demitri:** Supervision, **Mario Caironi:** Conceptualization, Supervision, Draft review, Funding acquisition.

Declaration of Competing Interest

The authors declare that they have no known competing financial interests or personal relationships that could have appeared to influence the work reported in this paper.

Data availability

Data will be made available on request.

Acknowledgment

L.L., P.C., I.I., and M.C. acknowledge the support of the European Research Council (ERC) under the European Union's Horizon 2020 research and innovation programme "ELFO", Grant Agreement No. 864299. P.C. acknowledges funding from the Marie Skłodowska-Curie actions (project name: BioConTact, Grant Agreement No. 101022279) under the European Union's Horizon 2020 research and innovation programme. M.C. and V.G. acknowledge partial support from the European Unions Horizon 2020 research and innovation programme, under Grant Agreement No. 964596 "ROBOFOOD". This work also received support under the European Union's Horizon 2020 research and innovation programme "GREENELIT", Grant Agreement No. 951747, and falls within the Sustainability Activity of Istituto Italiano di Tecnologia.

Appendix A. Supporting information

Supplementary data associated with this article can be found in the online version at doi:10.1016/j.nanoen.2023.108168.

References

[1] L. Lamanna, P. Cataldi, M. Friuli, C. Demitri, M. Caironi, Monitoring of drug release via intra body communication with an edible pill, Adv. Mater. Technol. 2200731 (2022).
[2] J. Kim, A.S. Campbell, B.E.-F. de Ávila, J. Wang, Wearable biosensors for healthcare monitoring, Nat. Biotechnol. 1 (2019).
[3] C. Steiger, et al., Ingestible electronics for diagnostics and therapy, Nat. Rev. Mater. 4 (2019) 83–98.
[4] L. Lamanna, et al., Flexible and transparent aluminum-nitride-based surface-acoustic-wave device on polymeric polyethylene naphthalate, Adv. Electron. Mater. 1900095 (2019).
[5] L. Piro, et al., Flexible SAW microfluidic devices as wearable pH sensors based on ZnO nanoparticles, Nanomaterials 11 (2021) 1479.
[6] M. Agostini, et al., Surface-acoustic-wave (SAW) induced mixing enhances the detection of viruses: application to measles sensing in whole human saliva with a SAW lab-on-a-chip, Adv. Funct. Mater. 2201958 (2022).
[7] J. Jiao, Q. Lu, Z. Wang, Y. Qin, X. Cao, Sandwich as a triboelectric nanogenerator, Nano Energy 79 (2021), 105411.
[8] Z. LináWang, Triboelectric nanogenerators as new energy technology and self-powered sensors–Principles, problems and perspectives, Faraday Discuss. 176 (2014) 447–458.
[9] M.B. Durukan, et al., Multifunctional and physically transient supercapacitors, triboelectric nanogenerators, and capacitive sensors, Adv. Funct. Mater. 32 (2022) 2106066.
[10] M. Bergmann, et al., Plastic pollution in the Arctic, Nat. Rev. Earth Environ. 3 (2022) 323–337.
[11] Y. Zhu, C. Romain, C.K. Williams, Sustainable polymers from renewable resources, Nature 540 (2016) 354–362.
[12] E. Stucchi, et al., Biodegradable all-polymer field-effect transistors printed on Mater-Bi, J. Inf. Disp. 22 (2021) 247–256.
[13] Cataldi, P. et al. An Electrically Conductive Oleogel Paste for Edible Electronics. *Advanced Functional Materials* **n/a**, 2113417, doi:https://doi.org/10.1002/adfm.202113417.
[14] A.S. Sharova, F. Melloni, G. Lanzani, C.J. Bettinger, M. Caironi, Edible electronics: the vision and the challenge, Adv. Mater. Technol. 6 (2021) 2000757.
[15] Y. Wu, et al., Edible and nutritive electronics: materials, fabrications, components, and applications, Adv. Mater. Technol. 5 (2020) 2000100.
[16] A.S. Sharova, M. Caironi, Sweet electronics: honey-gated complementary organic transistors and circuits operating in air, Adv. Mater. 33 (2021) 2103183.
[17] I.K. Ilic, et al., Self-powered edible defrosting sensor, ACS Sens. (2022).
[18] Shintake, J., Sonar, H., Piskarev, E., Paik, J. & Floreano, D. in 2017 IEEE/RSJ International Conference on Intelligent Robots and Systems (IROS). 6221–6226 (IEEE).
[19] L. Chambers, J. Winfield, I. Ieropoulos, J. Rossiter, in *Electroactive Polymer Actuators and Devices (EAPAD)*, SPIE,, 2014, pp. 46–51.
[20] W. Xu, et al., Food-based edible and nutritive electronics, Adv. Mater. Technol. 2 (2017) 1700181.
[21] L. Gibson, E.N. Wilman, W.F. Laurance, How green is 'green'energy? Trends Ecol. Evol. 32 (2017) 922–935.
[22] A. Midilli, I. Dincer, M. Ay, Green energy strategies for sustainable development, Energy Policy 34 (2006) 3623–3633.
[23] F.-R. Fan, Z.-Q. Tian, Z.L. Wang, Flexible triboelectric generator, Nano Energy 1 (2012) 328–334.
[24] C. Wu, A.C. Wang, W. Ding, H. Guo, Z.L. Wang, Triboelectric nanogenerator: a foundation of the energy for the new era, Adv. Energy Mater. 9 (2019) 1802906.
[25] H. Ouyang, et al., Self-powered pulse sensor for antidiastole of cardiovascular disease, Adv. Mater. 29 (2017) 1703456.
[26] Z. Li, G. Zhu, R. Yang, A.C. Wang, Z.L. Wang, Muscle-driven in vivo nanogenerator, Adv. Mater. 22 (2010) 2534–2537.
[27] J. Wang, F. Li, F. Zhu, O.G. Schmidt, Recent progress in micro-supercapacitor design, integration, and functionalization, Small Methods 3 (2019) 1800367.
[28] P. Huang, et al., On-chip and freestanding elastic carbon films for micro-supercapacitors, Science 351 (2016) 691–695.
[29] C. Gao, et al., A directly swallowable and ingestible micro-supercapacitor, J. Mater. Chem. A 8 (2020) 4055–4061.
[30] V. Orts Mercadillo, et al., Electrically Conductive 2D Material Coatings for Flexible and Stretchable Electronics: A Comparative Review of Graphenes and MXenes, Adv. Funct. Mater. 2204772 (2022).
[31] M. Kouhi, M.P. Prabhakaran, S. Ramakrishna, Edible polymers: an insight into its application in food, biomedicine and cosmetics, Trends Food Sci. Technol. 103 (2020) 248–263.
[32] W. Jiang, et al., Fully bioabsorbable natural-materials-based triboelectric nanogenerators, Adv. Mater. 30 (2018) 1801895.
[33] R. Guo, et al., Deep learning assisted body area triboelectric hydrogel sensor network for infant care, Adv. Funct. Mater. 2204803 (2022).
[34] A.P. Sathya Prasanna, et al., Green energy from edible materials: triboelectrification-enabled sustainable self-powered human joint movement monitoring, ACS Sustain. Chem. Eng. (2022).
[35] G. Khandelwal, N.P.M. Joseph Raj, N.R. Alluri, S.-J. Kim, Enhancing hydrophobicity of starch for biodegradable material-based triboelectric nanogenerators, ACS Sustain. Chem. Eng. 9 (2021) 9011–9017.
[36] G. Khandelwal, et al., All edible materials derived biocompatible and biodegradable triboelectric nanogenerator, Nano Energy 65 (2019), 104016.
[37] X. Wang, et al., Food-materials-based edible supercapacitors, Adv. Mater. Technol. 1 (2016) 1600059.
[38] D. Bresser, D. Buchholz, A. Moretti, A. Varzi, S. Passerini, Alternative binders for sustainable electrochemical energy storage–the transition to aqueous electrode processing and bio-derived polymers, Energy Environ. Sci. 11 (2018) 3096–3127.
[39] R. Hyppölä, I. Husson, F. Sundholm, Evaluation of physical properties of plasticized ethyl cellulose films cast from ethanol solution Part I, Int. J. Pharm. 133 (1996) 161–170.
[40] T. Kim, S.-H. Yi, S.-E. Chun, Electrophoretic deposition of a supercapacitor electrode of activated carbon onto an indium-tin-oxide substrate using ethyl cellulose as a binder, J. Mater. Sci. Technol. 58 (2020) 188–196.
[41] E.P. o F. Additives, et al., Re-evaluation of celluloses E 460 (i), E 460 (ii), E 461, E 462, E 463, E 464, E 465, E 466, E 468 and E 469 as food additives, EFSA J. 16 (2018), e05047.
[42] T. Wüstenberg, Cellulose and cellulose derivatives in the food industry: fundamentals and applications, John Wiley & Sons,, 2014.
[43] S. Kamel, N. Ali, K. Jahangir, S. Shah, A. El-Gendy, Pharmaceutical significance of cellulose: a review, Express Polym. Lett. 2 (2008) 758–778.
[44] C. Demitri, et al., Encapsulation of Lactobacillus kefiri in alginate microbeads using a double novel aerosol technique, Mater. Sci. Eng.: C. 77 (2017) 548–555.
[45] L. Lamanna, et al., Determination of absorption and structural properties of cellulose-based hydrogel via ultrasonic pulse-echo time-of-flight approach, Cellulose 25 (2018) 4331–4343, https://doi.org/10.1007/s10570-018-1874-4.
[46] E.P. o F. Additives, N.S. a t Food, Scientific opinion on the re-evaluation of vegetable carbon (E 153) as a food additive, EFSA J. 10 (2012) 2592.
[47] M. Absollhi, Encyclopedia of toxicology, Elsevier,, 2014.
[48] D. Cao, et al., Amphipathic Binder Integrating Ultrathin and Highly Ion-Conductive Sulfide Membrane for Cell-Level High-Energy-Density All-Solid-State Batteries, Adv. Mater. 33 (2021) 2105505.
[49] P. Cataldi, et al., Graphene–polyurethane coatings for deformable conductors and electromagnetic interference shielding, Adv. Electron. Mater. 6 (2020) 2000429.
[50] X. Wu, et al., Hybrid graphene/Carbon nanofiber wax emulsion for paper-based electronics and thermal management, Adv. Electron. Mater. 6 (2020) 2000232.

[51] E. Mahdi, A. Dean, The effect of filler content on the tensile behavior of polypropylene/cotton fiber and poly (vinyl chloride)/cotton fiber composites, Materials 13 (2020) 753.
[52] R.W. Rice, Mechanical properties of ceramics and composites: grain and particle effects, CRC Press,, 2000.
[53] D. Yang, et al., "Green" films from renewable resources: properties of epoxidized soybean oil plasticized ethyl cellulose films, Carbohydr. Polym. 103 (2014) 198–206.
[54] M. Davidovich-Pinhas, S. Barbut, A. Marangoni, The gelation of oil using ethyl cellulose, Carbohydr. Polym. 117 (2015) 869–878.
[55] T. Kulomaa, et al., Cellulose fatty acid esters as sustainable film materials–effect of side chain structure on barrier and mechanical properties, RSC Adv. 5 (2015) 80702–80708.
[56] C. Demitri, et al., Novel superabsorbent cellulose-based hydrogels crosslinked with citric acid, J. Appl. Polym. Sci. 110 (2008) 2453–2460.
[57] M. Hassan, N. Tucker, M.J. Le Guen, Thermal, mechanical and viscoelastic properties of citric acid-crosslinked starch/cellulose composite foams, Carbohydr. Polym. 230 (2020), 115675.
[58] U.S. Rashid, A.N. Bezbaruah, Citric acid modified granular activated carbon for enhanced defluoridation, Chemosphere 252 (2020), 126639.
[59] J.P. Chen, S. Wu, K.-H. Chong, Surface modification of a granular activated carbon by citric acid for enhancement of copper adsorption, Carbon 41 (2003) 1979–1986.
[60] M. Li, A. Pal, A. Aghakhani, A. Pena-Francesch, M. Sitti, Soft actuators for real-world applications, Nat. Rev. Mater. 7 (2022) 235–249.
[61] L. Lamanna, F. Rizzi, V.R. Bhethanabotla, M. De Vittorio, Conformable surface acoustic wave biosensor for E-coli fabricated on PEN plastic film, Biosens. Bioelectron. 112164 (2020).
[62] J. Kelleher, et al., Degradation of cellulose within the gastrointestinal tract in man, Gut 25 (1984) 811–815.
[63] M. Bryant, Cellulose digesting bacteria from human feces, Am. J. Clin. Nutr. 31 (1978) S113–S115.
[64] K. Yan, et al., A non-toxic triboelectric nanogenerator for baby care applications, J. Mater. Chem. A 8 (2020) 22745–22753.
[65] E. Josef, R. Yan, R. Guterman, M. Oschatz, Electrospun carbon fibers replace metals as a current collector in supercapacitors, ACS Appl. Energy Mater. 2 (2019) 5724–5733.
[66] Obreja, V.V. in *AIP Conference Proceedings*. 98–120 (American Institute of Physics).
[67] I.K. Ilic, E. Lepre, N. López-Salas, Caffeine-derived noble carbons as ball milling-resistant cathode materials for lithium-ion capacitors, ACS Appl. Mater. Interfaces 13 (2021) 29612–29618.
[68] Fluid, S.G. & In, T. (United States Pharmacopoeial Convention: Rockville, MD).